# Quantum chemical modelling, molecular docking, synthesis and experimental anti-microbial activity of 1,4-diazepan linked piperidine derivative

Khushbu Agrawal[1*], Tarun M. Patel[2], Shavi Thakur[1], Kruti Patel[1] and Sumit Mittal[3]

## Abstract

**Background**  In this work, we represent synthesis, in silico analysis and biological activity of 1,4 diazepine linked piperidine derivatives (6a–6o). All the derivatives were screened for their anti-microbial activity against gram-positive (*Staphylococcus aureus, Bacillus Subtills, Bacillus megaterium*) and gram-negative (*Escherichia coli, Pseudonymous, Shigella sp.*) bacteria. Compounds were synthesized from reaction of tert-butyl 1,4-diazepane-1-carboxylic, butyryl chloride and varied aromatic aldehyde, further characterized by $^1$H NMR and LCMS spectral techniques.

**Result**  Using ampicillin as a positive control, the synthetic compounds 6a–6o were tested for their in-silico study and experimental anti-microbial activity against gram-positive (*Staphylococcus aureus, Bacillus Subtills, Bacillus megaterium*) and gram-negative (*Escherichia coli, Pseudonymous, Shigella sp.*) bacteria. According to in vitro assay compound 6a, compound 6c, compound 6d, compound 6m and compound 6l showed higher activity against all the tested strains. Molecule 6i, compound 6j, compound 6k, compound 6f has good to moderate antibacterial activity. DFT computations were used to optimize the molecular geometry at the B3LYP/6-31G (d, p) theoretical level. The corresponding energy values of molecular orbitals were visualized using optimized geometries. Moreover, Auto Dock Vina 1.2.0 is used to assess molecular docking against two target proteins, Bacillus subtilis (PDB ID: 6UF6) and Protease Vulgaris (PDB ID: 5HXW). The target molecule 6b displayed the best binding energies for both. Additionally, we calculated the ADME for each molecule (6a–6o).

**Conclusion**  All fifteen synthesized compounds were screened for their in vitro and in silico analysis. In vitro analysis for anti-microbial activity was carried out against gram-positive (*Staphylococcus aureus, Bacillus Subtills, Bacillus megaterium*) and gram-negative (*Escherichia coli, Pseudonymous, Shigella sp.*) bacteria and compound 6a, compound 6c, compound 6d, compound 6m and compound 6l exhibits more potent activity towards all tested strains. Molecular docking is performed against target proteins, L-amino acid deaminase from *Proteus Vulgaris* and LcpA ligase from *Bacillus subtilis*, representing the Gram-negative bacterium and Gram-positive bacterium, respectively. Compound 6b showed the highest no. of interaction with protein according to molecular docking. With the advent of innovative techniques like ADME, we select their hit compounds early on and anticipate future pharmacokinetic and pharmacodynamic benefits and drawbacks of these promising therapeutic candidates.

**Keywords**  1,4 diazepan, Molecular docking, ADME calculation, DFT, Anti-microbial, SAR

---

*Correspondence:
Khushbu Agrawal
agrawalkhushbu007@gmail.com
Full list of author information is available at the end of the article

Agrawal *et al. Future Journal of Pharmaceutical Sciences*     (2024) 10:80

Page 2 of 17

**Graphical abstract**



## Background

Heterocycles are crucial chemicals their applications in many domains, including medicinal, agrochemical, and veterinary [1]. Several seven membered heterocyclic rings, with 2 hetero atoms, have shown wide range of medicinal activity. Among these, 1,4-diazepine,1,4-diazepane, and azepinone have been studied in detail. 1,4-diazepanes, also known as homopiperazine, hexahydro-1,4 diazepine, were first identified as a fundamental heterocyclic molecule in 1899. Later, a simple
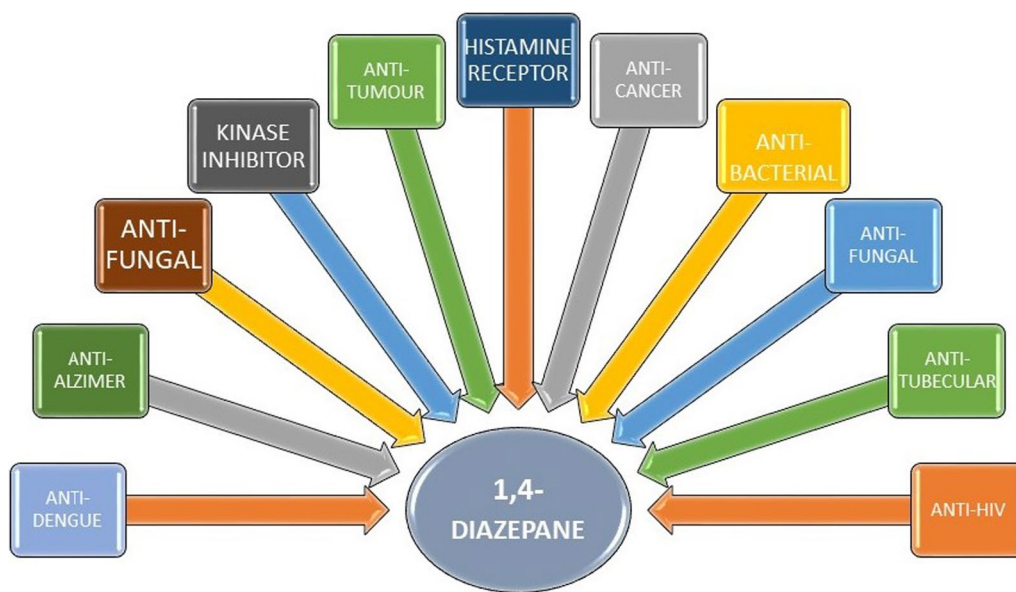


**Fig. 1** Different medicinal activity of 1,4 diazepane
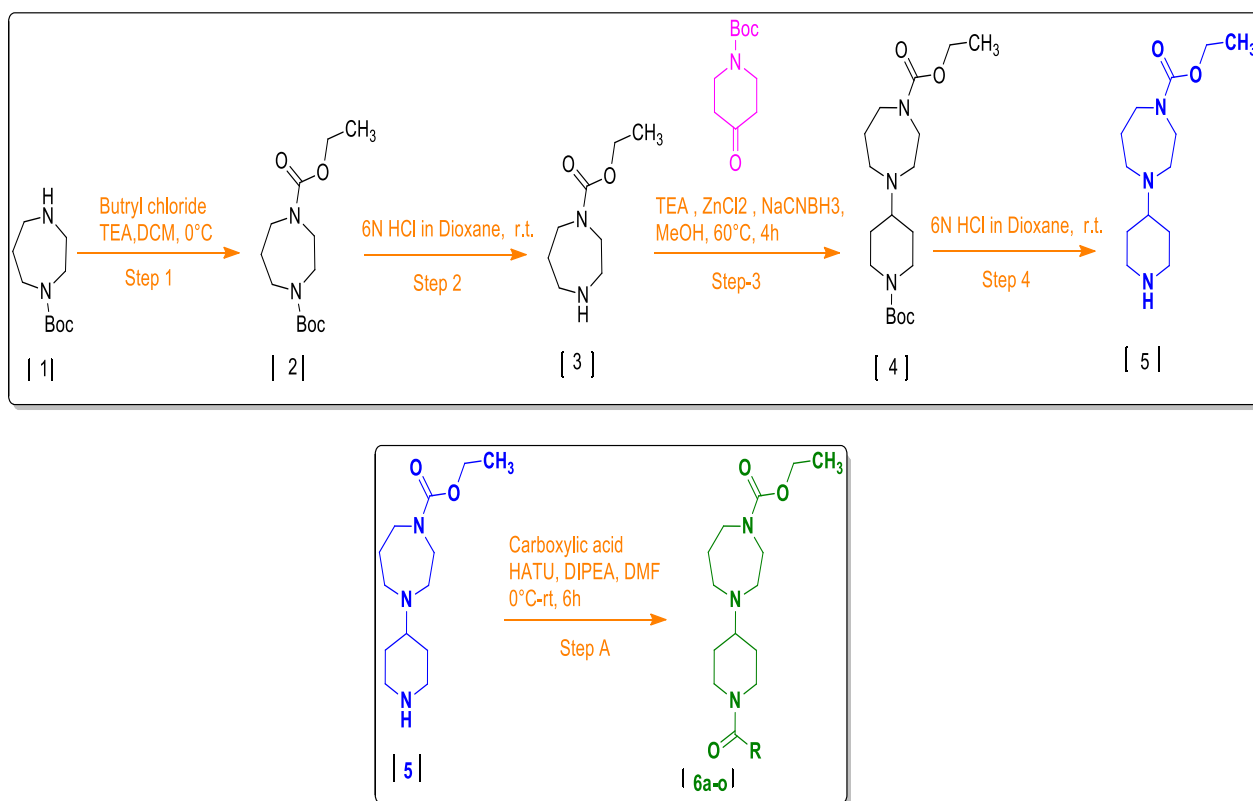
**Scheme 1** Synthetic route of 1,4 diazepane linked piperidine derivative

method was developed to manufacture these at industrial scale [2]. Molecular formula of 1,4 diazepane is $C_5H_{12}N_2$ and M.P. is 42 °C [3]. 1,4-diazepane is seven membered heterocyclic ring with nitrogen atoms at position 1 and position 4 of diazepan ring [4]. These molecules have been extensively studied owing to their versatile nature, and potential application in medicines, agrochemicals, and materials science [5]. Moreover, the 1,4-diazepane (homopiperazine) ring is prevalent among the various substitutions, linkers, as well as scaffolds used in pharmaceutical hit-to-lead optimization, particularly as a crucial component of optimized lead compounds [6]. Further, as 1,4-diazepane is hydrophobic, facilitate the organotin complex to permeate the cell and enhance the compound's biological activity [7]. In medicinal chemistry, 1,4-diazepane moiety has shown extensive pharmaceutical properties (Fig. 1) as anti-HIV [8, 9], anti-dengue [10], anti-Alzheimer [11], anti-tubercular [12], anti-fungal [13], anti-oxidant [14, 15], anti-bacterial [16], anti-cancer [17], anti-microbial

[13, 18], Histamine receptor [19], anti-tumour [7, 20], and as Kinase inhibitor [21].

Further, piperidine is a fundamental heterocyclic part of medical chemistry. Piperidine core compounds exhibit pharmaceutical properties like anti-HIV, anti-cancer. A.R. Zala and colleagues developed piperidine-containing molecules as antibacterial drugs in 2023 [22]. Mahmat Yildiz and colleagues developed piperidine derivatives that act as antimicrobial agents [23]. In contrast, Enrico Casalone and colleagues developed 1,4-diazepane derivatives as antimicrobial agents in 2020 [24]. Since, both piperidine and 1,4 diazepane show potent antimicrobial activities, in this study we created 1,4 diazepane linked piperidine derivatives and have characterize their antimicrobial efficacy. The derivative molecules have also been investigated using a series of computational chemistry tools, such as the Density Functional Theory, Molecular docking and ADME analysis. Here, we aim to facilitate the current research in designing innovative strategies for

Agrawal *et al. Future Journal of Pharmaceutical Sciences*     (2024) 10:80

Page 4 of 17

the discovery and development of good antimicrobial agents.

## Methods

All the compounds and solvents were purchased from Sigma Aldrich and used without any additional purification. The gradient of MeOH in MDC was created using the elutes and was used for the thin layer chromatography (TLC) method on silica gel plates (60F254, 0.2 mm thick, Merck). In this study, we used a Bruker Advance II 400 NMR spectrometer, used with the internal standard tetra methyl silane (TMS) as a $^1$H NMR spectrometer, to perform $^1$H NMR spectra in CDCl$_3$ solution at 400 MHz. Parts per million, or ppm, are used to compute the value in $^1$H NMR.

As the mobile phase of the LCMS equipment, which used WATERS to record data, 0.15% formic acid in acetonitrile was used as a mobile phase for the LCMS equipment.

### Chemistry

The five-step synthesis process outlined in Scheme 1 was created to produce the desired anti-microbial active ingredient. Commercially available tert-butyl 1,4-diazepane-1-carboxylic (**1**) intrigues the production route when it is coupled with butyryl chloride in the presence of triethanolamine (TEA) and methylene chloride (DCM) to produce compound **2** [25]. Compound **3** is produced by carbamate hydrolysis using compound **2** and 6 N HCl in dioxane to remove the boc protecting group [26]. In the presence of TEA, ZnCl$_2$, and MeOH, compound **4** was produced by treating compound **3** with commercially available tert-butyl-4-oxopiperidine-1-carboxylate[27]. Once more, carbamate hydrolysis is performed to remove the boc protecting group in preparation for the transition from compound **4** to compound **5** [26]**.** With the addition of DIPEA, the carboxylic acid in DMF was reacted with compound **5** in the presence of HATU and generated a high quality desired derivative (**6a-o**).[28, 29]. All the used aldehydes and properties of desired derivatives shown in Table 1**.**
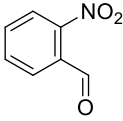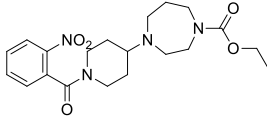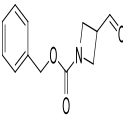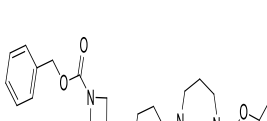
### In vitro assay
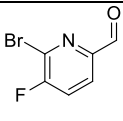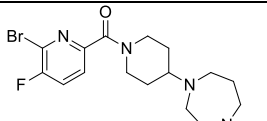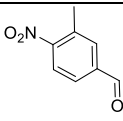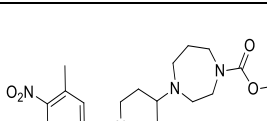
For the investigation of in vitro anti-microbial activity, the cup plate method [30, 31], which is very popular, was used. Gram-positive (*Staphylococcus aureus, Bacillus Subtills, Bacillus megaterium* and gram-negative (*Escherichia coli, Pseudonymous, Shigella* sp.) microorganisms, as well as Staphylococcus aureus (Gram +), were used to test in-vitro anti-microbial activity. To carry out this approach, all bacterial cultures were first kept in nutrient broth and then

incubated overnight at a temperature of 37 °C. A full hour was given for the incubated molten agar to set and solidify before it was transferred to the sterilized petri plates. Bacterial culture was evenly swabbed on the sterile plates using a cotton swab. On agar media, 6 mm broad bores were constructed using sterilized cork. Each bore was filled with the test compound solution, which had a measured concentration of 1000 μg/ml, using a sterile tip and micropipette. A plate was similarly prepared for the positive control ampicillin, which is taken as standard. The prepared plates were incubated for 24 h at 37 °C. Every bore had a clear zone encircling it after the incubation process, demonstrating tha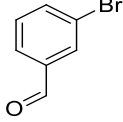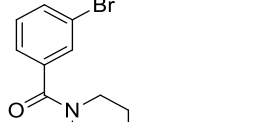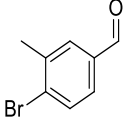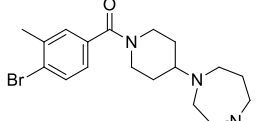t the 1,4-diazepane linked piperidine derivative under test had anti-microbial efficacy. The average diameter of these formed clear zones of inhibition was determined and used to report activity in millimeters. A value for the MIC (minimum inhibitory concentration) was obtained using the liquid dilution method [32], All derivatives MIC values were established for *Staphylococcus aureus* (Gram+) bacterium. The investigated substances were dissolved in a suitable solvent at a concentration of 50 mg/ml. Similar to this, a conventional ampicillin solution was made at a 50 mg/ml concentration. Bacterial culture inoculum preparation was carried out. In a series of test tubes, 0.2 ml of inoculum is inserted along with a 1 ml solution of the test substance at a specified concentration. In each test tube, 3.8 ml of sterile water was also added. All these test tubes were maintained under observation and incubated for a day in order to detect the existence of turbidity. A similar process was used to screen ampicillin, which is a commonly used medication. MIC values are those where bacterial growth was not seen to occur.
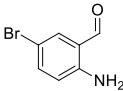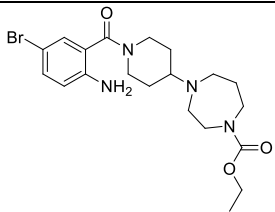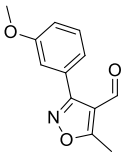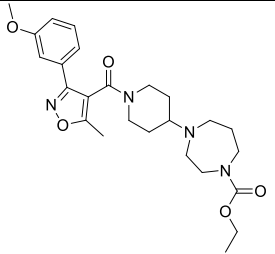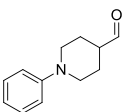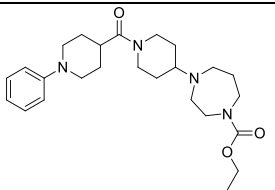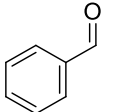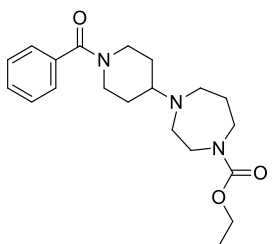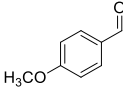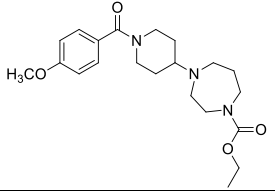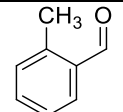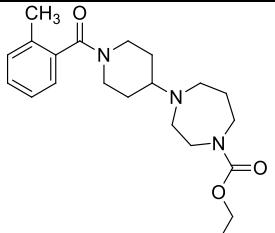
### Computational methods

The electronic structures of all 1,4 diazepane linked piperidine derivative molecules (**6a–6o**) were studied using quantum mechanical calculations. Each molecule was constructed using GaussView 5 software [33] and was subjected to geometry optimization using DFT calculations at the B3LYP/6-31G(d,p) level of theory as implemented in Gaussian 09 quantum chemistry package [34]. The calculations were performed in an implicit PCM water solvent model. No symmetrical constraints were imposed during the optimization. Optimized geometries were used to visualize molecular orbitals and their associated energy values using GaussView 5. In particular, the nature and energetics of the lowest unoccupied molecular orbital (LUMO) and highest occupied

Agrawal *et al. Future Journal of Pharmaceutical Sciences*      (2024) 10:80

Page 5 of 17
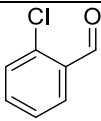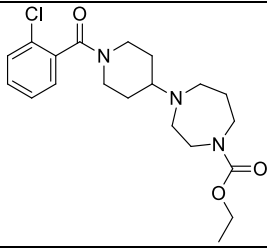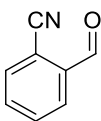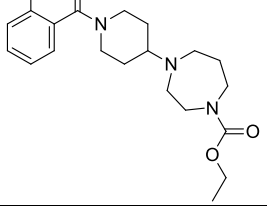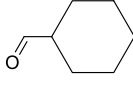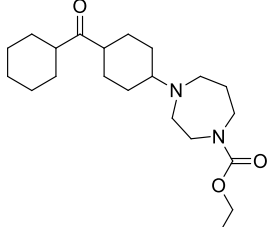
**Table 1** Properties of compounds

| Compound Number | Aldehyde used (R) | Name | Structure | M.W. |
|---|---|---|---|---|
| 6a | | ethyl 4-(1-(2-nitrobenzoyl)piperidin-4-yl)-1,4-diazepane-1-carboxylate | | 404.47 |
| 6b | | ethyl 4-(1-(1-((benzyloxy)carbonyl)azetidine-3-carbonyl)piperidin-4-yl)-1,4-diazepane-1-carboxylate | | 472.59 |
| 6c | | ethyl 4-(1-(6-bromo-5-fluoropicolinoyl)piperidin-4-yl)-1,4-diazepane-1-carboxylate | | 457.34 |
| 6d | | ethyl 4-(1-(3-methyl-4-nitrobenzoyl)piperidin-4-yl)-1,4-diazepane-1-carboxylate | | 418.49 |
| 6e | | ethyl 4-(1-(3-bromobenzoyl)piperidin-4-yl)-1,4-diazepane-1-carboxylate | | 438.37 |
| 6f | | ethyl 4-(1-(4-bromo-3-methylbenzoyl)piperidin-4-yl)-1,4-diazepane-1-carboxylate | | 452.38 |

**Table 1** (continued)

| | | | | |
|---|---|---|---|---|
| 6g | | ethyl 4-(1-(2-amino-5-bromobenzoyl)piperidin-4-yl)-1,4-diazepane-1-carboxylate | | 453.38 |
| 6h | | ethyl 4-(1-(3-(3-methoxyphenyl)-5-methylisoxazole-4-carbonyl)piperidin-4-yl)-1,4-diazepane-1-carboxylate | | 470.38 |
| 6i | | ethyl 4-(1-(1-phenylpiperidine-4-carbonyl)piperidin-4-yl)-1,4-diazepane-1-carboxylate | | 442.60 |
| 6j | | ethyl 4-(1-benzoylpiperidin-4-yl)-1,4-diazepane-1-carboxylate | | 359.47 |
| 6k | | ethyl 4-(1-(2-methylbenzoyl)piperidin-4-yl)-1,4-diazepane-1-carboxylate | | 389.49 |
| 6l | | ethyl 4-(1-(2-methylbenzoyl)piperidin-4-yl)-1,4-diazepane-1-carboxylate | | 373.49 |

**Table 1** (continued)

| | | | | |
|---|---|---|---|---|
| 6m |  | ethyl 4-(1-(2-chlorobenzoyl)piperidin-4-yl)-1,4-diazepane-1-carboxylate |  | 393.91 |
| 6n |  | ethyl 4-(1-(2-cyanobenzoyl)piperidin-4-yl)-1,4-diazepane-1-carboxylate |  | 383.48 |
| 6o |  | ethyl 4-(4-(cyclohexanecarbonyl)cyclohexyl)-1,4-diazepane-1-carboxylate |  | 364.52 |

molecular orbital (HOMO) were characterized. Several other molecular properties were calculated from the HOMO and LUMO energies, namely, the global hardness (η), softness (σ), electronegativity (χ), and electrophilicity index (ω). The following equations are used to compute these properties:

$$\chi = \frac{1}{2}(E_{HOMO} + E_{LUMO}) \tag{1}$$

$$\eta = -\frac{1}{2}(E_{HOMO} - E_{LUMO}) \tag{2}$$

$$\sigma = \frac{1}{\eta} \tag{3}$$

$$\omega = \frac{\mu^2}{2\eta} \tag{4}$$

Next, the optimized geometry of each derivative molecule was used to perform molecular docking against two target proteins corresponding to the *Protease Vulgaris* (PDB ID: 5HXW) [35] and *Bacillus subtilis* (PDB ID: 6UF6) [36]. The starting structure for the target proteins were based on their crystal structure deposited in the RCSB protein data bank. Both proteins were prepared for molecular docking by removing any existing ligand and

water molecules, followed by charge assignment using MGL Tools 1.5.7. [37] The grid box corresponding to the whole protein was defined for each target. Each derivative molecule was prepared for docking using MGL Tools 1.5.7. AutoDock Vina 1.2.0 [38] was used for docking the derivate molecules against the two target proteins. Ten conformations were generated for each derivative molecule and the most favorable conformation, based on the binding affinity, was selected for further structural analysis. The non-covalent interactions between the protein and docked ligand were analysed and visualized using LigPlot software [39].

Further, the Absorption, Distribution, Metabolism, and Excretion (ADME) analysis was carried out for each derivatized molecule using the SwissADME server [40] The ADME analysis provides determines various physiochemical properties to assess the pharmacodynamic properties of a potential ligand molecule. Various relevant parameters, such as the Lipinski's rule of five violations, number of hydrogen donors, hydrogen acceptors, rotatable bonds, total polar surface area, skin permeability (Log Kp), molar refractivity, gastrointestinal absorption (GI), blood brain barrier (BBB), inhibition of cytochromes P450 isoforms (CYP1A2, CYP2C19, CYP2C9, CYP2D6) were estimated.

Next, we carried out Quantitative Structure–activity relationships (QSAR) to determine the quantitative
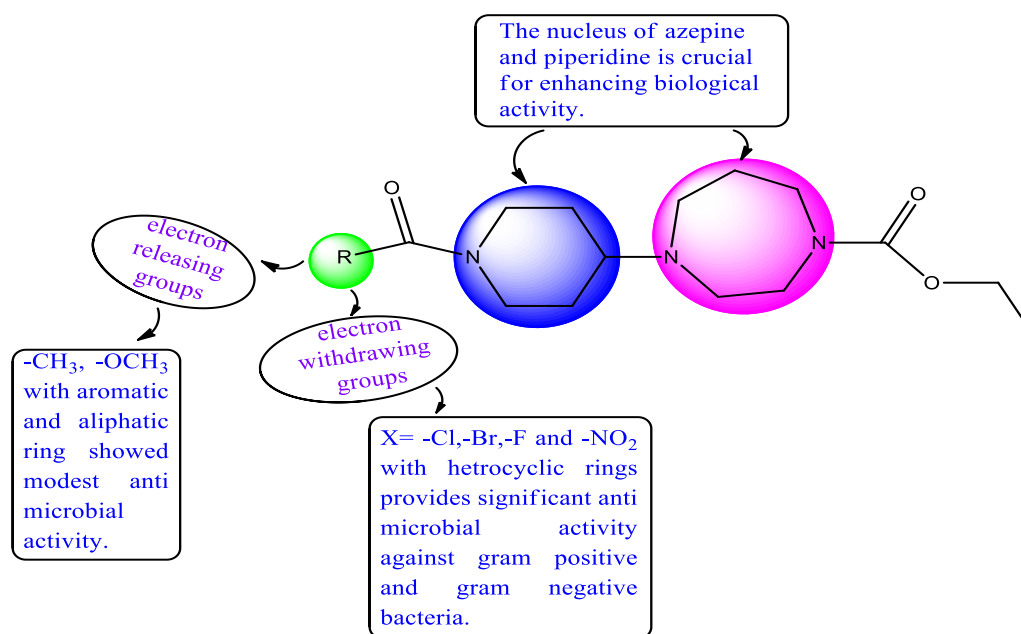
**Fig. 2** Structure activity relationship study

relationship between the biological activity and the molecule properties of the derivatives. We constructed the QSAR models by performing multiple linear regression analysis, which links selected independent variables with the dependent variable using the following equation:

**Table 2** Antibacterial activity of tested compounds as a zone of inhibition in MIC(μg/mL) of synthesized compound

| Compound number | *Staphylococcus aureus* (Gram+) | *Bacillus Subtills* (Gram+) | *Bacillus megaterium* (Gram+) | *Escherichia coli* (Gram−) | *Pseudonymous spp.* (Gram−) | *Shigella sp.* (Gram−) |
|---|---|---|---|---|---|---|
| **6a** | 46 | 42 | 44 | 37 | 39 | 20 |
| **6b** | 45 | 32 | 38 | 20 | 15 | – |
| **6c** | 59 | 54 | 48 | 50 | 51 | 33 |
| **6d** | 47 | 41 | 40 | 37 | 34 | 18 |
| **6e** | 51 | 46 | 45 | 42 | 29 | 22 |
| **6f** | 53 | 47 | 49 | 47 | 34 | 26 |
| **6g** | 51 | 45 | 45 | 41 | 35 | 21 |
| **6h** | 57 | 53 | 50 | 52 | 40 | 31 |
| **6i** | 47 | 36 | 40 | 23 | 19 | 8 |
| **6j** | 35 | 28 | – | 20 | 16 | – |
| **6k** | 40 | 34 | 37 | 25 | 21 | 11 |
| **6l** | 45 | 40 | 41 | 32 | 29 | 18 |
| **6m** | 58 | 50 | 52 | 47 | 39 | 28 |
| **6n** | 40 | 38 | 34 | 31 | 28 | 16 |
| **6o** | 30 | – | – | 17 | – | – |
| Ampicilin | 48 | 39 | 29 | 40 | 32 | 21 |

Where X i are the molecular descriptors, Y is the biological activity, n is number of descriptors, a 0 is the constant and a i are the respective coefficients.

## Result

By observing structural alterations brought on by the attachment of various substitutions and their placement on the heterocyclic ring in the generated derivative, the link between structure and activity was investigated (Fig. 2). Because of the varied positions of the aryl group and heterocyclic ring, biological activity was changing. In this study, different substituted phenyl rings linked to piperidine and piperidine directly coupled to 1,4-diazepane were found to have different anti-microbial activities. Distinct substitutions have distinct electrical properties, and these differences are shown in their anti-microbial effectiveness. According to research on SAR, anti-microbial activity can vary depending on the heterocyclic or aryl ring. The heterocyclic ring substitutions of manufactured compounds could either donate electrons or draw them out. When substitutions such halogenated groups at various positions on a heterocyclic ring are made, the anti-microbial action increases. According to Table 2, when phenyl rings are substituted in compounds with different halogenated groups, the chloro group exhibits more activity than the bromo group. The enhanced antimicrobial activity was found to be more in both **6c** and **6h**, due to the heterocyclic moiety in the synthetic derivatives with alkoxy phenyl ring in **6h** and the heterocyclic moiety on the heterocyclic ring with −Br and −F in **6c**. Higher antibacterial inhibitory action was demonstrated in **6m** by the phenyl ring with the chloro group in the ortho position. As opposed to the meta-substituted

**6e** and the amine-aryl ring with a bromine substitution in **6g**, the phenyl ring with a bromine and methyl group in **6f** shown stronger inhibitory activity. Higher antibacterial inhibitory action was demonstrated by compound **6a**'s phenyl ring with the nitro group in the ortho position as compared to compound **6d**'s phenyl ring with the electron-donating and withdrawing groups replaced. In contrast, **6l** had reduced activity due to the presence of an electron releasing group at the o-position. The methoxy group, a weak electron donor, was shown to be less active than other groups in position 4 of the phenyl ring in compound **6k**. Other substituted derivatives **6i**, **6b**, and **6j** displayed modest activity, while **6o** was found to be more effective than regular ampicillin against *Staphylococcus aureus* and *E. coli.*

Table 2 shows that the majority of the substances tested had varying inhibitory effects on the growth of the bacterial strains that were put to the test, according to the results of the study. Because the compound **6a**, the compound **6d**, and the compound **6m**, compound **6l** both possess electron withdrawing and electron releasing groups, these compounds showed a high level of inhibitory activity against the tested microbial strains. Comparatively to the reference drug Ampicillin, compound **6c** substituted with −Br and −F on its heterocyclic ring as well as compound **6h** containing heterocyclic rings attached to methoxybenzene were found to exhibit superior activity against all Gram-positive and Gram-negative microbial strains. Even though compound **6o** showed no effect against *B. subtilis, Bacilius magneterium, Pseudomonas spp., and Shigella spp.*, compound **6j** lost its antibacterial efficacy due to the absence of an aryl ring substitution. Due to the presence of an electron
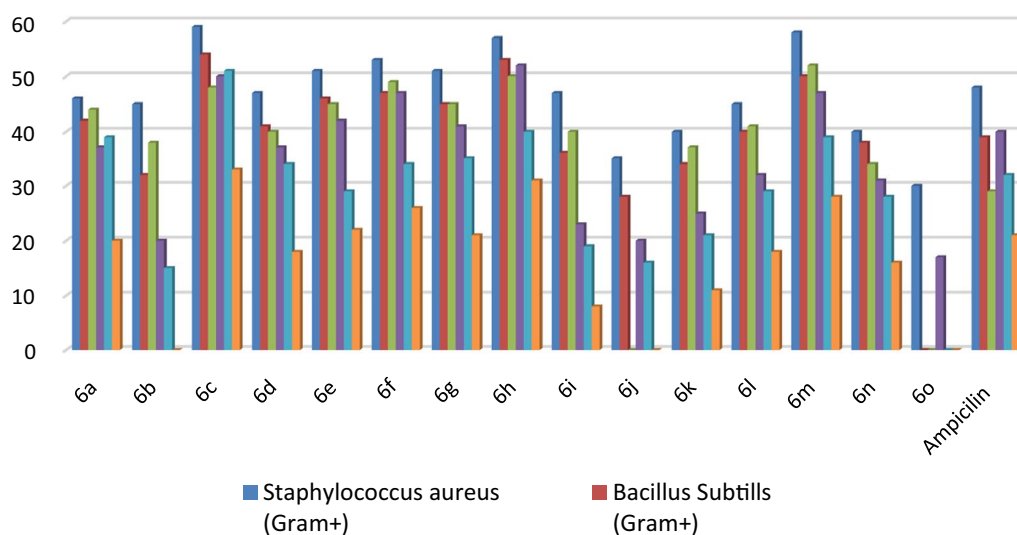


**Fig. 3** Statistical diagram of antimicrobial activity
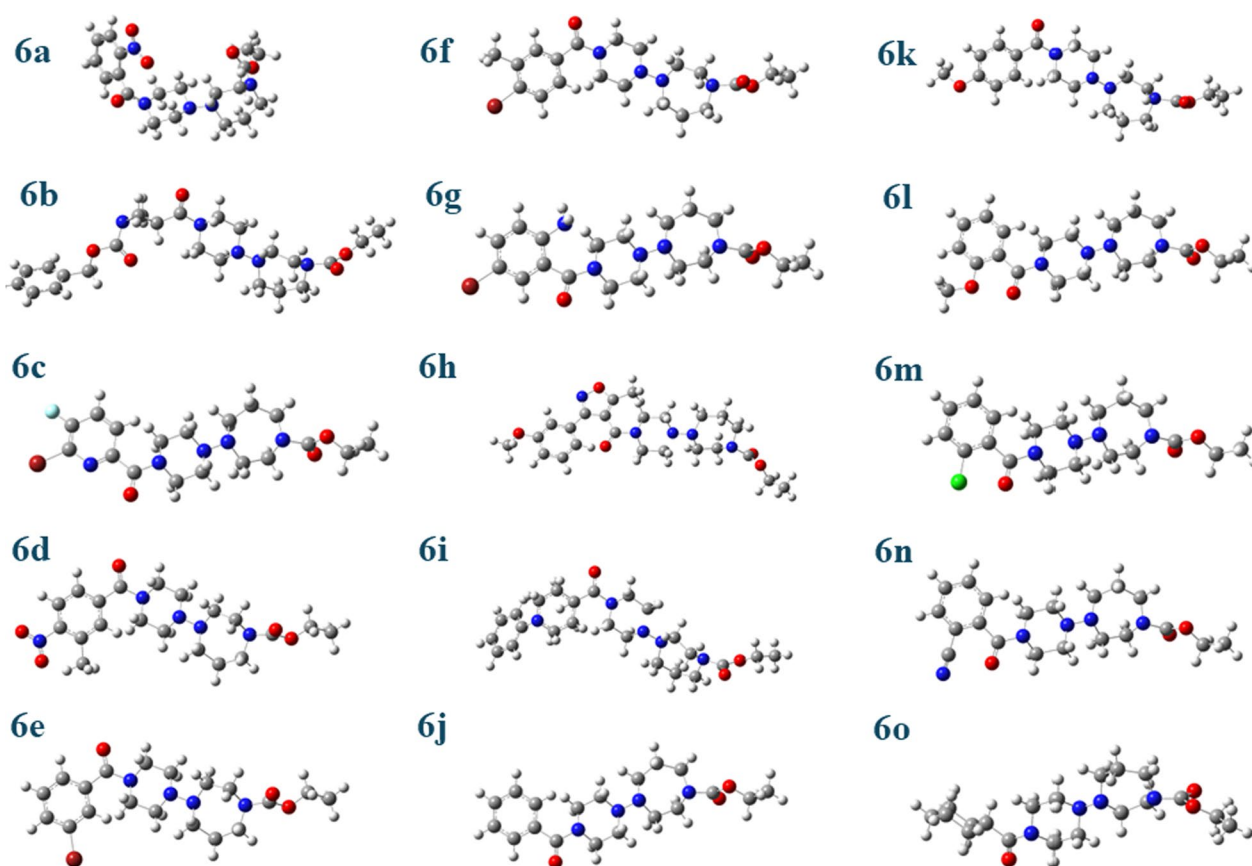
**Fig. 4** The geometry of 1,4 diazepane linked piperidine derivative molecules optimized at the B3LYP/6-31G(d,p) level of theory

**Table 3** The calculated $E_{HOMO}$, $E_{LUMO}$ (eV), $E_{HOMO}$—$E_{LUMO}$ ($\Delta E$, eV), electronegativity ($\chi$), chemical potential ($\mu$), global hardness ($\eta$), global softness ($\sigma$), and global electrophilicity index ($\omega$) for derivative molecules as calculated at the B3LYP/6-31G(d,p) level of theory

| No | $E_{HOMO}$ (eV) | $E_{LUMO}$ (eV) | $E_{HOMO}$−$E_{LUMO}$ (eV) | $\chi$ (eV) | $\eta$ (eV) | $\sigma$ (eV$^{-1}$) | $\omega$ (eV) |
|---|---|---|---|---|---|---|---|
| **6a** | − 0.3340 | 0.0365 | − 0.3706 | − 0.1487 | 0.1853 | 5.3971 | 0.0597 |
| **6b** | − 0.3058 | 0.1265 | − 0.4323 | − 0.0896 | 0.2162 | 4.6264 | 0.0186 |
| **6c** | − 0.3131 | 0.0574 | − 0.3706 | − 0.1278 | 0.1853 | 5.3974 | 0.0441 |
| **6d** | − 0.3134 | 0.0276 | − 0.3410 | − 0.1429 | 0.1705 | 5.8649 | 0.0599 |
| **6e** | − 0.3080 | 0.0770 | − 0.3850 | − 0.1155 | 0.1925 | 5.1951 | 0.0346 |
| **6f** | − 0.3083 | 0.0779 | − 0.3862 | − 0.1152 | 0.1931 | 5.1788 | 0.0343 |
| **6g** | − 0.2912 | 0.0794 | − 0.3705 | − 0.1059 | 0.1853 | 5.3981 | 0.0303 |
| **6h** | − 0.2892 | 0.0519 | − 0.3412 | − 0.1187 | 0.1706 | 5.8620 | 0.0413 |
| **6i** | − 0.2460 | 0.1148 | − 0.3608 | − 0.0656 | 0.1804 | 5.5428 | 0.0119 |
| **6j** | − 0.3052 | 0.0873 | − 0.3926 | − 0.1089 | 0.1963 | 5.0946 | 0.0302 |
| **6k** | − 0.3056 | 0.0899 | − 0.3955 | − 0.1078 | 0.1977 | 5.0571 | 0.0294 |
| **6l** | − 0.3029 | 0.0902 | − 0.3931 | − 0.1064 | 0.1965 | 5.0879 | 0.0288 |
| **6m** | − 0.3076 | 0.0766 | − 0.3842 | − 0.1155 | 0.1921 | 5.2051 | 0.0347 |
| **6n** | − 0.3105 | 0.0586 | − 0.3691 | − 0.1259 | 0.1846 | 5.4184 | 0.0430 |
| **6o** | − 0.3049 | 0.0601 | − 0.3650 | − 0.1224 | 0.1825 | 5.4789 | 0.0410 |
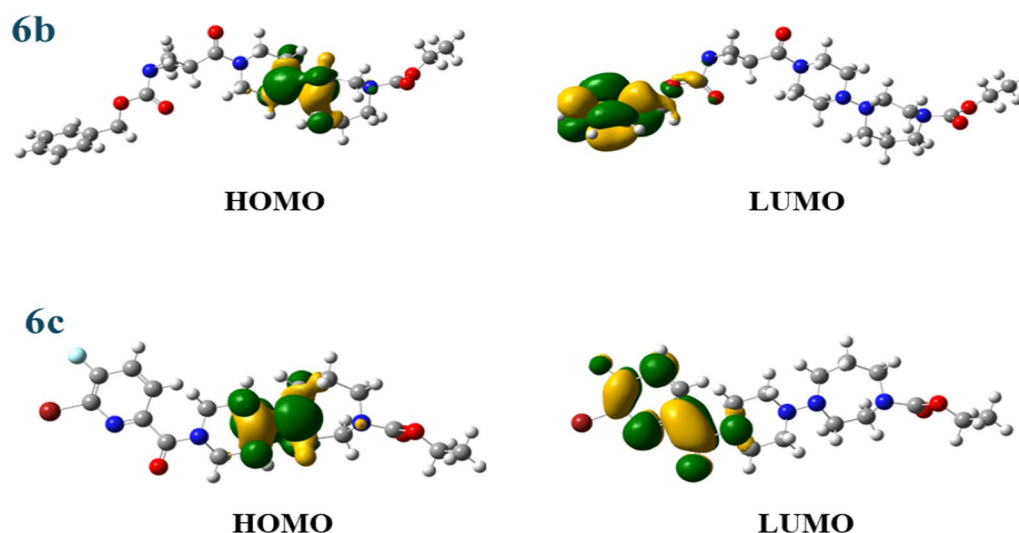
**Fig. 5** The HOMO and LUMO orbitals for selected derivative molecules (**6b** and **6c**) as calculated at the B3LYP/6-31G(d,p) level of theory

releasing group and a phenyl ring, **6i, 6k** demonstrated a modest amount of inhibitory action against the investigated strains of *Pseudomonas spp., B. subtilis, E. coli,* and *Staphylococcus aureus*. Figure 3 depicts the graphical representation of antibacterial activity.

### DFT calculations

All 1,4 diazepane linked piperidine derivative molecules were optimized using the DFT methods at the B3LYP/6-31G(d,p) level of theory. The optimized geometries are shown in Fig. 4 and the various electronic properties are presented in Table 3. First, we compared the energy gap ($E_{HOMO}$-$E_{LUMO}$), which is an important parameter to assess the thermal stability and the chemical reactivity of a molecule. The $E_{HOMO}$ and $E_{LUMO}$ energy gap were computed to be negative for all derivative molecules, indicating their stability and in the following order: **6b > 6k > 6l > 6j > 6f > 6e > 6m > 6a > 6c > 6g > 6n > 6o > 6i > 6h > 6d**. Further, Frontier Molecular Orbital analysis illustrate that for all molecules, the lowest occupied molecular orbital (LUMO) orbital is localized on the π orbitals of the phenyl ring (Fig. 5). Whereas the highest occupied molecular orbital (HOMO) orbital is localized on the diazepane and piperidine binding site. We also computed additional electronic and structural parameters, such as electronegativity (χ), global hardness (η), global softness (σ) and global electrophilicity index (ω), to ascertain the biological activity of the derivative molecules (Table 3). The large χ and ω for all compounds indicate their excellent bioactivity.

### Molecular docking

The derivative molecules were next subjected to molecular docking to assess their antibacterial potential. To this

**Table 4** Calculated docking affinities (in kcal/mol) of the derivative molecules and ampicillin against the target proteins from *Bacillus subtilis* (PDB ID: 6UF6), and *Proteus Vulgaris* (PDB ID: 5HXW)

| No | 5HXW | 6UF6 |
|---|---|---|
| **6a** | − 8.7 | − 7.7 |
| **6b** | − 9.4 | − 8.2 |
| **6c** | − 8.8 | − 7.4 |
| **6d** | − 8.3 | − 7.2 |
| **6e** | − 8.1 | − 7 |
| **6f** | − 8.1 | − 7.3 |
| **6g** | − 8.1 | − 6.9 |
| **6h** | − 8.2 | − 7.1 |
| **6i** | − 8.0 | − 7.1 |
| **6j** | − 8.6 | − 6.8 |
| **6k** | − 8.4 | − 6.9 |
| **6l** | − 8.3 | − 7.2 |
| **6m** | − 8.3 | − 6.9 |
| **6n** | − 8.5 | − 7 |
| **6o** | − 8.1 | − 6.9 |
| Ampicillin | − 7.8 | − 6.9 |

end, we used the geometry optimized derivative molecules to perform molecular docking against two target proteins, L-amino acid deaminase from *Proteus Vulgaris* and LcpA ligase from *Bacillus subtilis*, representing the Gram-negative bacterium and Gram-positive bacterium, respectively. The relative stability of the target protein – ligand complex was determined by their binding affinities Table 4 and their intermolecular interactions with the target proteins (Additional file 1: Figures S21–S22).
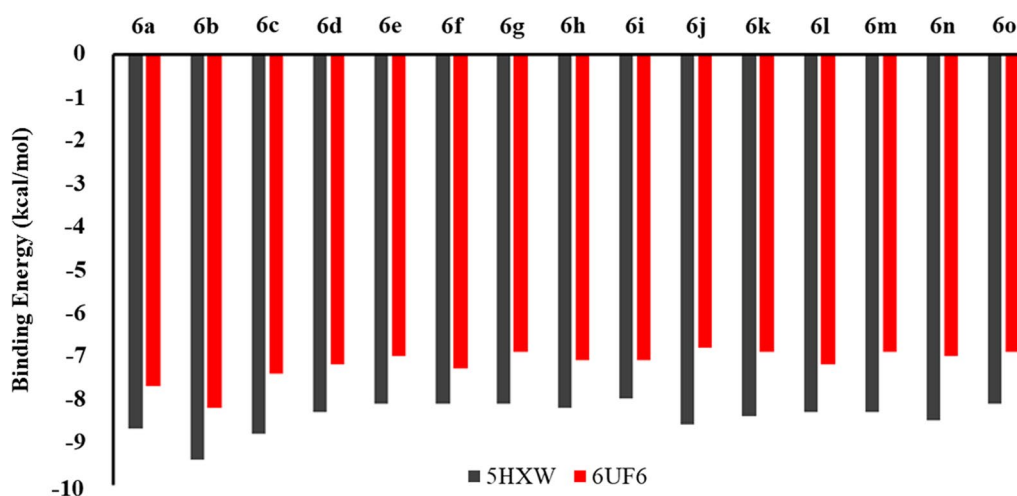
**Fig. 6** Comparison of the calculated docking affinities (in kcal/mol) of all derivative molecules and ampicillin against the target proteins from *Bacillus subtilis* (PDB ID: 6UF6), and *Proteus Vulgaris* (PDB ID: 5HXW)
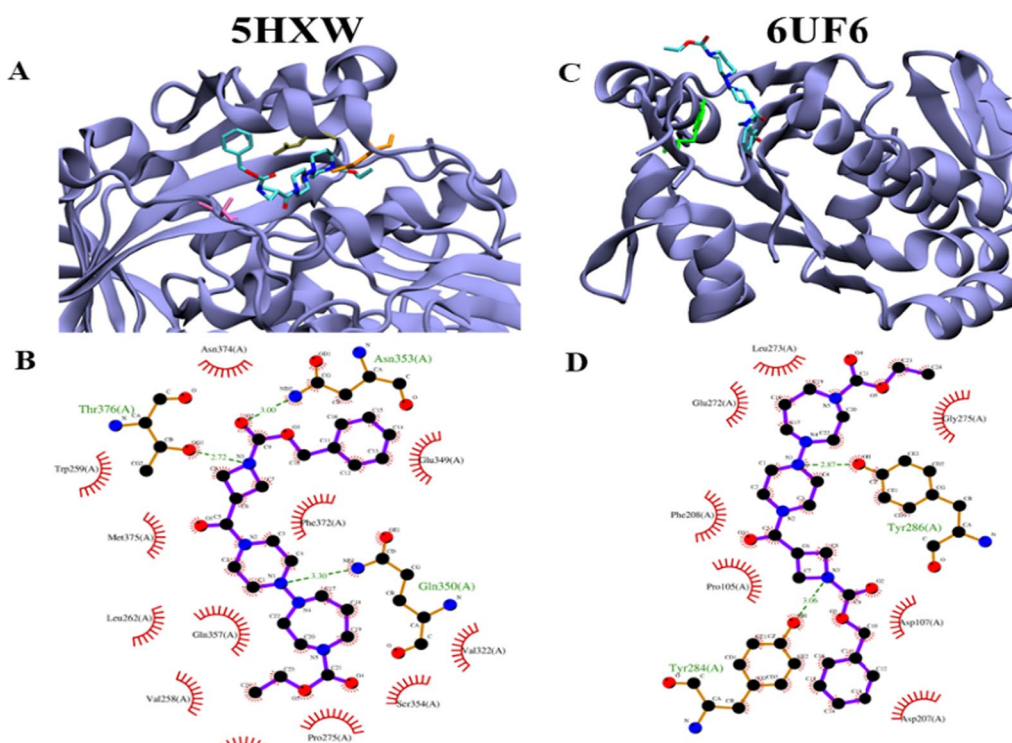


**Fig. 7** Overlay of the protein-derivative molecule 6b complexes as obtained from their docking with *Bacillus subtilis* (PDB ID: 6UF6) and *Proteus Vulgaris* (PDB ID: 5HXW) proteins. The docked poses were chosen based on their binding affinities and geometric similarities. Intermolecular interactions between the derivation molecules and the target proteins are shown. The hydrogen bond interactions are highlighted

Molecules **6b** showed the largest binding affinity for both target proteins (Fig. 6). Further analysis of the protein–ligand complex revealed a higher number of interactions in the case of **6b** (Fig. 7). The derivate **6b** formed H-bonds involving residues Tyr286 and Tyr284 of the L-amino acid deaminase from *Proteus Vulgaris*. Similarly, it formed H-bonds with Asn353 and Gln350 residues of LcpA ligase from *Bacillus subtilis*. These H-bonds, together with several hydrophobic interactions, provide higher binding strength to the complex of **6b** with target proteins.

**Table 5** Drug-likeness predictions for the derivative molecules as computed using SwissADME

| C | MW | NRB | NHA | NHD | TPSA | LogP | LV | MR |
|---|---|---|---|---|---|---|---|---|
| **6a** | 405.45 | 7 | 7 | 0 | 102.15 | 0.98 | 0 | 123.03 |
| **6b** | 473.57 | 9 | 7 | 0 | 85.87 | 1.28 | 0 | 144.39 |
| **6c** | 458.33 | 6 | 7 | 0 | 69.22 | 1.87 | 0 | 119.66 |
| **6d** | 419.47 | 7 | 7 | 0 | 102.15 | 1.31 | 0 | 127.99 |
| **6e** | 439.35 | 6 | 5 | 0 | 56.33 | 2.18 | 0 | 121.9 |
| **6f** | 453.37 | 6 | 5 | 0 | 56.33 | 2.5 | 0 | 126.87 |
| **6g** | 454.36 | 6 | 5 | 1 | 82.35 | 1.78 | 0 | 126.31 |
| **6h** | 475.58 | 8 | 9 | 2 | 89.98 | 1.18 | 0 | 145.88 |
| **6i** | 445.6 | 10 | 5 | 0 | 59.57 | 2.25 | 0 | 142.45 |
| **6j** | 360.45 | 6 | 5 | 0 | 56.33 | 1.56 | 0 | 114.2 |
| **6k** | 390.48 | 7 | 6 | 0 | 65.56 | 1.57 | 0 | 120.7 |
| **6l** | 390.48 | 7 | 6 | 0 | 65.56 | 1.35 | 0 | 120.7 |
| **6m** | 394.9 | 6 | 5 | 0 | 56.33 | 2.07 | 0 | 119.21 |
| **6n** | 385.46 | 6 | 6 | 0 | 80.12 | 1.33 | 0 | 118.92 |
| **6o** | 366.5 | 6 | 5 | 0 | 56.33 | 1.76 | 0 | 116.22 |

The number of rotatable bonds (NRB), number of hydrogen donors (NHD), number of hydrogen acceptors (NHA), total polar surface area (TPSA) in $Å^2$, LogP value and Lipinski's rule of five violation (LV), and Molar Refractivity (MR) are reported

**Table 6** Absorption, Distribution, Metabolism, and Excretion (ADME) analysis for the derivative molecules as computed using SwissADME

| | Log $K_p$ | GI Absorption | BBB Absorption | Inhibitor interaction | | | |
|---|---|---|---|---|---|---|---|
| | | | | CYP1A2 | CYP2C19 | CYP2C9 | CYP2D6 |
| **6a** | −7.6 | High | No | No | Yes | No | No |
| **6b** | −8.27 | High | No | No | Yes | No | No |
| **6c** | −7.53 | High | No | No | Yes | No | No |
| **6d** | −7.42 | High | No | No | Yes | Yes | No |
| **6e** | −7.19 | High | Yes | No | Yes | No | Yes |
| **6f** | −7.02 | High | Yes | No | Yes | No | Yes |
| **6g** | −7.37 | High | No | No | Yes | No | Yes |
| **6h** | −8.19 | High | No | No | No | No | Yes |
| **6i** | −6.99 | High | Yes | No | No | No | Yes |
| **6j** | −7.21 | High | No | No | Yes | No | No |
| **6k** | −7.4 | High | No | No | Yes | No | No |
| **6l** | −8.03 | High | No | No | No | No | No |
| **6m** | −6.97 | High | Yes | No | Yes | No | Yes |
| **6n** | −7.56 | High | No | No | Yes | No | No |
| **6o** | −6.94 | High | No | No | No | No | No |

Skin permeability (Log $K_p$), gastro-intestinal absorption (GI), blood brain barrier (BBB), and inhibition of cytochrome-P isoforms are reported

### ADME calculations

Next, we performed the ADME calculations for the derivative molecules using the SwissADME server to characterize their drug-likeness and bioavailability. The ADME analysis showed that none of the molecules violated any of the five Lipinski rule. (Table 5) Therefore, these molecules have good potential to be developed as orally active drugs. The TPSA value, closely related to the bioavailability, for the molecules were observed in the range of 56 $Å^2$ to 102 $Å^2$, which is well below the limit of 140 $Å^2$. Similarly, the number of rotatable bonds (NRB) for all molecules is less than the limit of 10, except for **6i**, suggesting that the molecules are conformationally stable.

Moreover, the low skin permeability value (Log $K_p$) for all molecules indicates low level of skin permeation (Table 6). All derivative molecules showed high level of gastrointestinal (GI) absorption. The molecule's hazardous or adverse effects also depend on its suppression of cytochromes P450 isoforms (CYP1A2, CYP2C19, CYP2C9, and CYP2D6). SwissADME predictions showed that all the derivative molecules show inhibition propensity against one or more of these isoforms.

Considering all the ADME predictions as well as the binding affinities, molecule **6b** appear as the most effective lead as an antibacterial agent. While it is noted that other derivative molecules, such as 6n, showed high binding affinity and similar binding mode as 6b, the latter is more favourable owing to its higher tendency to form H-bonds with the nearby receptor residues.

Among the 15 molecular descriptors, seven were selected for the regression analysis based on their correlation coefficient values. The seven descriptors are the following: Log P, Log S, NHA, η, molecular weight (MW), TPSA, and Log Kp. The resulting QSAR model based on the regression analysis is given by the following equation:

Where $N = 15$, $R = 0.87$, determination coefficient ($R^2$) $= 0.77$, mean square error (MSE) $= 1.77$, statistical confidence degree (F) $= 5.68$.

The high values of R2 and F indicate that the derived QSAR model is acceptable, and that the biological activity is linear correlated with these descriptors (Additional file 1: Figure S23). These descriptors can be used to predict inhibitory activity of new compounds based on the structure of 1,4 diazepane linked piperidine derivatives.

## Discussion

### Preparation of tert-butyl 4-butyryl-1,4-diazepane-1-carboxylate (2)

Tert-butyl 1,4-diazepane-1-carboxylate **(1)** (1.0 g, 4.99 mmol), TEA (1.04 mL, 7.48 mmol), and DCM (10 mL) were dissolved at 0 °C in a reaction jar. After then, the solution received a dropwise addition of butyryl chloride (798.0 mg, 7.48 mmol). The mixture was then mixed at room temperature for 30 min. The reaction mixture was then split equally between 100 mL of $H_2O$ and 100 mL of EtOAc. EtOAc ($2 \times 50$ mL) was used to extract the aqueous layer further. $Na_2SO_4$ was used to mix and dry the organic layers. Tert-butyl 4-Butyryl-1,4-diazepane-1-carboxylate **(2)** (1.2 g, 88.88%) was obtained as the crude product after the solvent was removed under vacuum. The next stage didn't require any purification because the crude product was used immediately.

### Preparation of 1-(1,4-diazepan-1-yl)butan-1-one hydrochloride salt (3)

The reaction mixture was agitated at room temperature for 16 h with tert-butyl 4-butyryl-1,4-diazepane-1-carboxylate **(2)** (1.0 g, 3.70 mmol) in 6N HCl-dioxane (10.0 mL). To produce the crude product, 1-(1,4-diazepan-1-yl)butan-1-one hydrochloride salt **(3)** (550 mg), the reaction mixture was then concentrated under vacuum. The crude product was utilized right away in the subsequent step of the reaction without going through any purifying procedures.

### Preparation of ethyl 4-(1-(tert-butoxycarbonyl) piperidin-4-yl)-1,4-diazepane-1-carboxylate (4)

Tert-butyl 4-oxopiperidine-1-carboxylate (578 mg, 2.90 mmol), 1-(1,4-diazepan-1-yl)butan-1-one hydrochloride salt **(3)** (500 mg, 2.90 mmol), TEA (1.2 mL, 8.70 mmol), $ZnCl_2$ (8.0 mg, 0.1 mmol), and MeOH (7 mL) were mixed in an RBF. The mixture for the reaction was heated to 60 °C and given 4 h to react. The reaction mixture was then cooled to zero degrees Celsius. $NaCNBH_3$ (540 mg, 8.70 mmol) was added to the reaction mixture at 0 °C, and the mixture was stirred for 16 h as it warmed to room temperature. A residue was produced after the reaction mixture was concentrated under a vacuum. The aqueous layer was extracted with EtOAc (250 mL) after the residue was divided between 500 mL of $H_2O$ and 500 mL of EtOAc. $Na_2SO_4$ was used to mix and dry the organic layers. A crude product was produced after the solvent was subsequently extracted under a vacuum. Column chromatography was used to purify the crude product. Ethyl 4-(1-(tert-butoxy carbonyl)piperidin-4-yl)-1,4-diazepane was the pure product that was produced. 400 mg of − 1-carboxylate **(4)**, 38.76% yield.

### Ethyl 4-(piperidin-4-yl)-1,4-diazepane-1-carboxylate hydrochloride salt (5)

The reaction mixture was agitated at room temperature for 16 h with ethyl 4-(1-(tert-butoxycarbonyl)piperidin-4-yl)-1,4-diazepane-1-carboxylate **(4)** (400 mg, 3.70 mmol) in 6N HCl-dioxane (4 mL). A crude product of ethyl 4-(piperidin-4-yl)-1,4-diazepane-1-carboxylate hydrochloride salt **(5)** (250 mg, 76.13% yield) was produced when the mixture was concentrated under vacuum. The crude product was utilized right away in the subsequent step of the reaction without going through any purifying procedures.

### General procedure of compound (6a–o)

The carboxylic acid (1 equivalent) was mixed in DMF (10 volumes) in a reaction vessel. Next, the resulting

mixture was cooled to absolute zero. After adding HATU (1.5 equivalents), the reaction mixture was stirred at 0 °C for 10 min. Ethyl 4-(piperidin-4-yl)-1,4-diazepane-1-carboxylate hydrochloride salt **(5)** (1.1 equivalents) and DIPEA (3 equivalents) were then added to the reaction mixture. The end product was stirred at room temperature for six hours. The reaction mixture was then dumped into ice-cold water after it had finished. The resultant residue was divided between 500 mL of $H_2O$ and 500 mL of EtOAc. EtOAc (250 mL) was used to extract the aqueous layer further. $Na_2SO_4$ was used to mix and dry the organic layers. The crude product was then produced after the solvent was removed under vacuum. To produce the final chemicals **6a-o**, column chromatography was used to purify the crude product. (Supplementary File).

### Ethyl 4-(1-(2-nitrobenzoyl) piperidin-4-yl)-1,4-diazepane-1-carboxylate (6a)

*¹H NMR (400 MHz, DMSO)* δ 1.25–1.29 (3H, t), 1.81 (4H, m), 2.77 (6H, m), 3.06 (2H, m), 3.49 (5H, m), 4.12–4.18 (2H, q), 4.77–4.88 (2H, m), 7.3 (1H, m), 7.57–7.61 (1H, m), 7.72 (1H, m), 8.21–8.23 (2H, d, J=8 Hz). LCMS m/z Cal. [M+H]⁺ 404.21 found [M+H]⁺405.21.

### Ethyl 4-(1-(1-((benzyloxy)carbonyl)azetidine-3-carbonyl) piperidin-4-yl)-1,4-diazepane-1-carboxylate (6b)

*¹H NMR (400 MHz, DMSO)* δ 0.85–0.96 (4H, m), 1.27–1.30 (4H, m), 2.00 (2H, m), 2.57–2.63 (1H, t, J=24 Hz), 2.78–2.90 (3H, m), 3.00 (2H, s), 3.49–3.55 (6H, m), 4.16–4.17 (6H, d, J=4 Hz), 4.77 (1H, s), 5.11 (2H, s), 7.28–7.37 (5H, m). LCMS m/z Cal. [M+H]⁺ 472.27 found [M+H]⁺473.2.

### Ethyl 4-(1-(6-bromo-5-fluoropicolinoyl) piperidin-4-yl)-1,4-diazepane-1-carboxylate (6c)

*¹H NMR (400 MHz, DMSO)* δ 1.29–1.32 (4H, m), 1.49–1.55 (2H, s), 1.67–1.72 (2H, m), 2.00 (4H, s), 2.81–2.97 (3H, m), 3.11–3.22 (2H, m), 3.53–3.61 (1H, m), 3.67 (3H, s), 4.18–4.20 (2H, d, J=8 Hz), 4.79–4.83 (1H, d, J=16 Hz), 7.55–7.58 (1H, t, J=12 Hz), 7.72–7.75 (1H, m). LCMS m/z Cal. [M-H]⁻ 458.12 found [M-H]⁻457.6.

### Ethyl 4-(1-(3-methyl-4-nitrobenzoyl) piperidin-4-yl)-1,4-diazepane-1-carboxylate (6d)

*¹H NMR (400 MHz, DMSO)* δ 1.23–1.34 (3H, m), 1.42–1.58 (4H, m), 2.01–2.31 (4H, m), 2.64 (3H, s), 2.82–2.90 (1H, d), 3.15–3.23 (4H, m), 3.43–3.46 (1H, m), 3.51–3.57 (2H, s), 3.72–3.79 (2H, m), 4.13–4.18 (2H, m), 4.83 (1H, s), 7.28 (1H, s), 7.34–7.40 (1H, m), 8.00–8.02 (1H, d, J=8 Hz). LCMS m/z Cal. [M+H]⁺ 418.22 found [M+H]⁺419.2.

### Ethyl 4-(1-(3-bromobenzoyl) piperidin-4-yl)-1,4-diazepane-1-carboxylate (6e)

*¹H NMR (400 MHz, DMSO)* δ 1.26–1.29 (3H, t, J=12 Hz), 1.48–1.53 (4H, m), 1.88 (4H, s), 2.80 (4H, d), 3.03 (1H, s), 3.16–3.22 (1H, m), 3.50–3.59 (2H, m), 3.70–3.77 (2H, m), 4.13–4.18 (2H, m), 4.76 (1H, s), 7.23–7.33 (2H, m), 7.55–7.58 (2H, d, J=12 Hz). LCMS m/z Cal. [M-2+H]⁻ 438.13 found [M+H]⁻405.21.

### Ethyl 4-(1-(4-bromo-3-methylbenzoyl) piperidin-4-yl)-1,4-diazepane-1-carboxylate (6f)

*¹H NMR (400 MHz, DMSO)* δ 1.26–1.30 (3H, t, J=16 Hz), 1.47–1.52 (4H, m), 1.87–1.99 (2H, m), 2.10 (3H, m), 2.44 (3H, s), 2.93–2.98 (4H, m), 3.51–3.54 (4H, m), 3.65 (1H, m), 4.15–4.17 (2H, m), 4.80–4.90 (1H, s), 7.08 (1H, s), 7.20–7.28 (1H, s), 7.57–7.59 (1H, d, J=8 Hz). LCMS m/z Cal. [M-H]⁻ 453.15 found [M-H]⁻452.0.

### Ethyl 4-(1-(2-amino-5-bromobenzoyl) piperidin-4-yl)-1,4-diazepane-1-carboxylate (6 g)

*¹H NMR (400 MHz, DMSO)* δ 1.29–1.32 (4H, m), 1.60–1.63 (4H, m), 2.01 (4H, s), 2.88–2.94 (6H, d, J=24 Hz), 3.16–3.17 (1H, d, J=4 Hz), 3.53–3.76 (2H, m), 4.16–4.21 (2H, m), 4.33 (2H, s), 6.64–6.66 (1H, d, J=8 Hz), 7.20 (1H, s), 7.30 (1H, s). LCMS m/z Cal. [M+H]⁺ 452.14 found [M+H]⁺453.2.

### Ethyl 4-(1-(3-(3-methoxyphenyl)-5-methylisoxazole-4-carbonyl) piperidin-4-yl)-1,4-diazepane-1-carboxylate (6h)

*¹H NMR (400 MHz, DMSO)* δ 0.88–0.92 (4H, m), 1.30 (8H, s), 2.32–2.75 (6H, m), 3.48 (4H, s), 3.69 (1H, s), 3.87–3.90 (2H, d, J=12 Hz), 4.17–4.18 (2H, d, J=4 Hz), 4.82 (1H, s), 7.04 (1H, s), 7.24–7.42 (3H, m). LCMS m/z Cal. [M+H]⁺ 470.25found [M+H]⁺471.2.

### Ethyl 4-(1-(1-phenylpiperidine-4-carbonyl) piperidin-4-yl)-1,4-diazepane-1-carboxylate (6i)

*¹H NMR (400 MHz, DMSO)* δ 1.28–1.32 (3H, m), 1.53 (4H, m), 1.81–1.84 (3H, m), 1.91–1.98 (7H, m), 2.52–2.60 (1H, m), 2.73–2.79 (1H, m), 2.84–2.98 (3H, m), 3.04–3.11 (1H, t, J=28 Hz), 3.16–3.22 (1H, m,), 3.51–3.52 (2H, m), 3.55 (1H, m), 3.70–3.77 (2H, m), 4.02–4.05 (1H, m), 4.13–4.18 (2H, m), 4.73–4.76 (1H, d, J=12 Hz), 6.87 (1H, s), 6.95–6.97 (2H, m), 7.26–7.28 (2H, m). LCMS m/z Cal. [M+H]⁺ 442.29 found [M+H]⁺442.60.

### Ethyl 4-(1-benzoylpiperidin-4-yl)-1,4-diazepane-1-carboxylate (6j)

*¹H NMR (400 MHz, DMSO)* δ 1.29–1.33 (3H, t, J=12 Hz), 1.47–1.72 (2H, m), 2.23–2.26 (3H, d, J=12 Hz), 2.43 (3H, s), 3.15–3.25 (3H, m), 3.62 (4H, s), 3.93 (3H, s), 4.19–4.22

Agrawal *et al. Future Journal of Pharmaceutical Sciences*   (2024) 10:80

Page 16 of 17

(2H, t, $J = 12$ Hz), 7.31–7.45 (6H, m). LCMS m/z Cal. $[M+H]^+$ 359.22 found $[M+H]^+$ 359.47.

## Conclusion

In this research study, synthesis, characterization, in silico and anti-microbial activity been done on a series of 1,4-diazepane linked piperidine derivatives. In vitro assay for anti-microbial activity done with Gram-positive (*Staphylococcus aureus, Bacillus Subtills, Bacillus megaterium*) and gram-negative (*Escherichia coli, Pseudonymous, Shigella* sp.) bacterial strains of synthesized compounds were compared to that of standard drug ampicillin and found to have good activity. The geometry optimization in gas phase at the B3LYP/6-31G (d,p) level of theory as implemented in Gaussian 05 DFT study. The negative values of EHOMO and ELUMO calculations for all derivative indicate their stability which favors for the chemical reactivity. The molecular docking against target proteins, L-amino acid deaminase from *Proteus Vulgaris* and LcpA ligase from *Bacillus subtilis* in identifying the relative stability of the target protein—ligand complex. Molecules **6b** showed the largest binding affinity for both target proteins. Also, the ADME predictions for each derivatized molecule favors for the highest binding affinity. Additional electronic properties, such as electronegativity (χ), global hardness (η), global softness (σ) and global electrophilicity index (ω), was computed to ascertain the biological activity of the derivative.

## Abbreviations

| | |
|---|---|
| M.P | Melting point |
| MeOH | Methanol |
| TLC | Thin Layer Chromatography |
| LCMS | Liquid chromatography-mass spectrometry. |
| TEA | Triethanolamine |
| DCM | Methylene Chloride |
| DIPEA | N,N-Diisopropylethylamine |
| DMF | N,N-Dimethylformamide |
| HATU | Hexafluorophosphate Azabenzotriazole Tetramethyl Uronium |
| MIC | Minimum inhibition concentration |
| HOMO | Highest occupied molecular orbital |
| LOMO | Lowest unoccupied molecular orbital |
| ADME | Absorption, Distribution, Metabolism, and Excretion |

## Supplementary Information

The online version contains supplementary material available at https://doi.org/10.1186/s43094-024-00652-y.

> **Additional file 1**.

## Author contributions
KA and TMP: conceptualization, Methodology writing, Data curation, editing. ST and KP: In vitro biological activity, writing, editing. SM: Software, Formal analysis, writing.

## Availability of data and materials
Data and materials are available upon request.

## Declarations

### Ethics approval and consent to participate
Not applicable.

### Consent for publication
Not applicable.

### Competing interests
There are no competing interests to declare for all authors.

### Author details
[1]Department of Chemistry, Shree Maneklal M. Patel Institute of Sciences and Research, Sector 15/23, Kadi Sarva Vishwavidyalaya, Gandhinagar, Gujarat 382023, India. [2]Department of Chemistry, Sir P. T. Science College Modasa, HNGU, Modasa, India. [3]School of Advanced Sciences and Languages (SASL), VIT Bhopal University Kothri Kalan, Near Indore Road, Bhopal, Madhya Pradesh 466114, India.

## References

1. Qadir T, Amin A, Sharma PK, Jeelani I, Abe H (2022) A review on medicinally important heterocyclic compounds. Open Med Chem J 16:1–34. https://doi.org/10.2174/18741045-v16-e2202280
2. Aitken RA, Sonecha DK, Slawin AMZ (2021) Homopiperazine (hexahydro-1,4-diazepine). Molbank. https://doi.org/10.3390/M1200
3. Bykov AV, Shestimerova TA, Bykov MA, Belova EV, Goncharenko VE, Dorovatovskii PV et al (2023) New lead-free hybrid halometallates with dioctahedral anions synthesized using the template function of homopiperazine. Russ Chem Bull 72:167–176. https://doi.org/10.1007/s11172-023-3721-5
4. Vessally E, Hosseinian A, Edjlali L, Bekhradnia A, Esrafili MD (2016) New route to 1,4-oxazepane and 1,4-diazepane derivatives: Synthesis from: N-propargylamines. RSC Adv 6:99781–99793. https://doi.org/10.1039/c6ra20718a
5. Zeynali H, Keypour H, Hosseinzadeh L, Gable RW (2021) The non-templating synthesis of macro-cyclic Schiff base ligands containing pyrrole and homopiperazine and their binuclear nickel(II), cobalt(II) and mononuclear platinum(II) complexes: X-ray single crystal and anticancer studies. J Mol Struct 1244:130956. https://doi.org/10.1016/j.molstruc.2021.130956
6. Ryan JH, Hyland C, Meyer AG, Smith JA, Yin J (2012) Chapter 7—seven-membered rings. In: Gribble GW (ed) Joule JABT-P in HC. Elsevier, pp 493–536
7. Shehata MR, Shoukry MM, Abdel Wahab AM (2021) Equilibrium studies of binary and mixed-ligand dimethyltin(IV) complexes involving homopiperazine and DNA constituents with reference to the antitumor activity. Phys Chem Liq 59:523–536. https://doi.org/10.1080/00319104.2020.1752689
8. Tret'yakova EV, Ma X, Kazakova OB, Shtro AA, Petukhova GD, Klabukov AM et al (2022) Synthesis and evaluation of diterpenic Mannich bases as antiviral agents against influenza A and SARS-CoV-2. Phytochem Lett 51:91–96. https://doi.org/10.1016/j.phytol.2022.07.010

9. Kobayakawa T, Yokoyama M, Tsuji K, Fujino M, Kurakami M, Onishi T et al (2023) Low-molecular-weight anti-HIV-1 agents targeting HIV-1 capsid proteins. RSC Adv 13:2156–2167. https://doi.org/10.1039/D2RA06837K

10. Smirnova I, Petrova A, Giniyatullina G, Smirnova A, Volobueva A, Pavlyukova J et al (2022) Synthesis, anti-influenza H1N1 and anti-dengue activity of a-ring modified oleanonic acid polyamine derivatives. Molecules 27:8499. https://doi.org/10.3390/molecules27238499

11. Abdollahi-Moghadam M, Keypour H, Azadbakht R, Koolivand M (2023) An experimental and theoretical study of a new sensitive and selective Al$^{3+}$ Schiff base fluorescent chemosensor bearing a homopiperazine moiety. J Mol Struct 1273:134289. https://doi.org/10.1016/j.molstruc.2022.134289

12. Srinivasarao S, Nandikolla A, Suresh A, Van CK, De Voogt L, Cappoen D et al (2020) Seeking potent anti-tubercular agents: Design and synthesis of substituted-: N-(6-(4-(pyrazine-2-carbonyl)piperazine/homopiperazine-1-yl)pyridin-3-yl)benzamide derivatives as anti-tubercular agents. RSC Adv 10:12272–12288. https://doi.org/10.1039/d0ra01348j

13. Abdel Wahab A, Shoukry M, Shehata MR, Khalf-Alla P (2022) Synthesis, equilibria, Dft and biological investigation of homopiperazine complex with diphenyltin(IV). Egypt J Chem 65:687–699. https://doi.org/10.21608/ejchem.2021.109334.4987

14. Aidi M, Keypour H, Shooshtari A, Mahmoudabadi M, Bayat M, Ahmadvand Z et al (2019) Synthesis of two new symmetrical macroacyclic Schiff base ligands containing homopiperazine moiety and their mononuclear complexes: Spectral characterization, X-ray crystal structural, antibacterial activities, antioxidant effects and theoretical studies. Polyhedron 167:93–102. https://doi.org/10.1016/j.poly.2019.02.030

15. Keypour H, Aidi M, Mahmoudabadi M, Karamian R, Asadbegy M, Gable RW (2019) Synthesis, X-ray crystal structural, antioxidant and antibacterial studies of new Cu(II) macroacyclic Schiff base complex with a ligand containing homopiperazine moiety. J Mol Struct 1198:126666. https://doi.org/10.1016/j.molstruc.2019.06.024

16. Meanwell NA, Loiseleur O (2022) Applications of isosteres of piperazine in the design of biologically active compounds: part 1. J Agric Food Chem 70:10942–10971. https://doi.org/10.1021/acs.jafc.2c00726

17. Asong GM, Voshavar C, Amissah F, Bricker B, Lamango NS, Ablordeppey SY (2022) An evaluation of the anticancer properties of SYA014, a homopiperazine-oxime analog of haloperidol in triple negative breast cancer cells. Cancers 14:6047. https://doi.org/10.3390/cancers14246047

18. Mantipally M, Gangireddy MR, Gundla R, Badavath VN, Mandha SR, Maddipati VC (2019) Rational design, molecular docking and synthesis of novel homopiperazine linked imidazo[1,2-a]pyrimidine derivatives as potent cytotoxic and antimicrobial agents. Bioorg Med Chem Lett 29:2248–2253. https://doi.org/10.1016/j.bmcl.2019.06.031

19. Szczepanska K, Kuder K, Kiec-Kononowicz K (2017) Histamine H3 receptor ligands in the group of (homo)piperazine derivatives. Curr Med Chem 25:1609–1626. https://doi.org/10.2174/0929867325666171123203550

20. Kraft O, Hoenke S, Csuk R (2022) A tormentic acid-homopiperazine-rhodamine B conjugate of single-digit nanomolar cytotoxicity and high selectivity for several human tumor cell lines. Eur J Med Chem Reports 5:100043. https://doi.org/10.1016/j.ejmcr.2022.100043

21. Gomi N, Shibuya K, Kawamura K, Kabeya M (2022) Synthesis of oxidative metabolites of K-115, a novel Rho-kinase inhibitor. Tetrahedron Lett 91:153589. https://doi.org/10.1016/j.tetlet.2021.153589

22. Zala AR, Rajani DP, Kumari P (2023) Design, synthesis, molecular docking and in silico ADMET investigations of novel piperidine-bearing cinnamic acid hybrids as potent antimicrobial agents. J Iran Chem Soc 20:1843–1856. https://doi.org/10.1007/s13738-023-02801-1

23. Yıldız M, Yıldırım H, Bayrak N, Çakmak SM, Mataracı-Kara E, Özbek-Çelik B et al (2023) Design, synthesis, in vitro and in silico characterization of plastoquinone analogs containing piperidine moiety as antimicrobial agents. J Mol Struct 1277:134845. https://doi.org/10.1016/j.molstruc.2022.134845

24. Casalone E, Vignolini T, Braconi L, Gardini L, Capitanio M, Pavone FS et al (2020) 1-benzyl-1,4-diazepane reduces the efflux of resistance-nodulation-cell division pumps in Escherichia coli. Future Microbiol 15:987–999. https://doi.org/10.2217/fmb-2019-0296

25. Pola S, Shah SR, Pingali H, Zaware P, Thube B, Makadia P et al (2021) Discovery of a potent G-protein-coupled receptor 119 agonist for the treatment of type 2 diabetes. Bioorg Med Chem 35:116071. https://doi.org/10.1016/j.bmc.2021.116071

26. Yukawa T, Nakada Y, Sakauchi N, Kamei T, Yamada M, Ohba Y et al (2016) Design, synthesis, and biological evaluation of a novel series of peripheral-selective noradrenaline reuptake inhibitors—part 3. Bioorg Med Chem 24:3716–3726. https://doi.org/10.1016/j.bmc.2016.06.014

27. O'brien DL, Whitem CB (2018) Piperidin-1-yl and azepin-1-yl carboxylates as muscarinic M4 receptor agonists US10030012B2, 24 July 2018

28. Guedes de La Cruz G, Svobodova B, Lichtenegger M, Tiapko O, Groschner K, Glasnov T (2017) Intensified microwave-assisted n-acylation procedure—synthesis and activity evaluation of TRPC3 channel agonists with a 1,3-dihydro-2H-benzo[d]imidazol-2-one core. Synlett 28:695–700. https://doi.org/10.1055/s-0036-1589472

29. Reddy DR, Linda W et al (2016) 1, 4-substituted piperidine derivatives. WO: CEPHALON INC OP—US 201562181384 P, 18 June 2016

30. Rohini R, Reddy PM, Shanker K, Kanthaiah K, Ravinder V, Hu A (2011) Synthesis of mono, bis-2-(2-arylideneaminophenyl) indole azomethines as potential antimicrobial agents. Arch Pharm Res 34:1077–1084. https://doi.org/10.1007/s12272-011-0705-z

31. Rohini R, Muralidhar Reddy P, Shanker K, Hu A, Ravinder V (2010) Antimicrobial study of newly synthesized 6-substituted indolo[1,2-c]quinazolines. Eur J Med Chem 45:1200–1205. https://doi.org/10.1016/j.ejmech.2009.11.038

32. Shanker K, Rohini R, Ravinder V, Reddy PM, Ho Y-P (2009) Ru(II) complexes of $N_4$ and $N_2O_2$ macrocyclic Schiff base ligands: their antibacterial and antifungal studies. Spectrochim Acta A Mol Biomol Spectrosc 73:205–211. https://doi.org/10.1016/j.saa.2009.01.021

33. Nielsen AB, Holder AJ (2009) Gauss view 5.0, user's reference. GAUSSIAN Inc, Pittsburgh

34. Frisch MJ, Trucks GW, Schlegel HB, Scuseria GE, Robb MA, Cheeseman JR et al (2009) Gaussian 09, Revision B.01. Gaussian 09, Revised B01, Gaussian, Inc, Wallingford CT, pp 1–20

35. Ju Y, Tong S, Gao Y, Zhao W, Liu Q, Gu Q et al (2016) Crystal structure of a membrane-bound l-amino acid deaminase from Proteus vulgaris. J Struct Biol 195:306–315. https://doi.org/10.1016/j.jsb.2016.07.008

36. Li FKK, Rosell FI, Gale RT, Simorre J-P, Brown ED, Strynadka NCJ (2020) Crystallographic analysis of Staphylococcus aureus LcpA, the primary wall teichoic acid ligase. J Biol Chem 295:2629–2639. https://doi.org/10.1074/jbc.RA119.011469

37. Sanner MF (1999) Python: a programming language for software integration and development. J Mol Graph Model 17:57–61

38. Eberhardt J, Santos-Martins D, Tillack AF, Forli S (2021) AutoDock Vina 1.2.0: new docking methods, expanded force field, and python bindings. J Chem Inf Model 61:3891–3898. https://doi.org/10.1021/acs.jcim.1c00203

39. Laskowski RA, Swindells MB (2011) LigPlot+: multiple ligand-protein interaction diagrams for drug discovery. J Chem Inf Model 51:2778–2786. https://doi.org/10.1021/ci200227u

40. Daina A, Michielin O, Zoete V (2017) SwissADME: a free web tool to evaluate pharmacokinetics, drug-likeness and medicinal chemistry friendliness of small molecules. Sci Rep 7:42717. https://doi.org/10.1038/srep42717

## Publisher's Note